Applied Surface Science 517 (2020) 146200

Contents lists available at ScienceDirect

Applied Surface Science

journal homepage: www.elsevier.com/locate/apsusc

Full Length Article

CO_2 hydrogenation to formic acid over platinum cluster doped defective graphene: A DFT study

Ge Yan[a], Zhengyang Gao[a,*], Mingliang Zhao[a], Weijie Yang[a,*], Xunlei Ding[b]

[a] School of Energy and Power Engineering, North China Electric Power University, Baoding 071003, China
[b] School of Mathematics and Physics, North China Electric Power University, Beijing 102206, China

ARTICLE INFO

Keywords:
CO_2 hydrogenation
Platinum cluster
Catalytic reduction
Density functional theory

ABSTRACT

The hydrogenation of CO_2 to formic acid is an important reaction in environmental catalysis, which can both alleviate the greenhouse effect and produce useful chemicals. Platinum element catalysts need to be investigated to realize large-scale development due to the expensive and scarce features. In this work, CO_2 hydrogenation to formic acid over Pt_4 cluster doped single-vacancy graphene was investigated using density functional theory. Catalyst configuration was optimized to perform corresponding gas adsorption and reduction reaction. Four reaction pathways were explored according to the reaction mechanism of Langmuir-Hinshelwood (L-H), Eley-Rideal (E-R) and termolecular Eley-Rideal (TER). Kinetic analysis was used to evaluate the reaction rate of different processes under the given temperature range, and the potential effect of CO molecule was also considered to better understand the feasibility. Results showed that Pt_4/SV was a stable and high activity catalyst. The minimum activation energy among different pathways was 0.56 eV and TER could be the dominant reaction mechanism of CO_2 hydrogenation. This work not only provides a promising catalyst but also gives a more deep understanding of CO_2 reduction technology and the future applicability of platinum metal catalysts.

1. Introduction

Fossil fuels, such as coal, natural gas, and oil, have been used as reliable, cheap and efficient energy sources [1]. However, with the rapid development of modern industry, due to the burning of fossil fuels, the carbon dioxide emitted by human beings to the atmosphere increases at a rate of 4% per year. The Met Office predicts that the average concentration of carbon dioxide will reach 411 ppm in 2019 [2]. It is of great discussion that CO_2 is used as a cheap and abundant feedstock to produce fuels and chemicals, and the most common conversion is the catalytic hydrogenation of CO_2 [3–5]. It can not only reduce greenhouse gas emissions but also obtain products with high industrial added value, which has significant environmental and economic benefits [6,7]. One important idea is the hydrogenation of CO_2 to formic acid (HCOOH). Formic acid is an important chemical substance used in making various compounds such as animal feeds and food preservatives [8,9]. Because CO_2 is a highly oxidized, thermodynamically stable compound, the utilization requires reaction with certain high energy substances or electroconductive processes [5]. The biggest challenge about CO_2 hydrogenation is the low activity and efficiency of catalysts due to the high chemical stability of CO_2 itself [10–12].

Nowadays, size-selected subnanometer transition metal clusters have gained lots of attention due to the special electronic and catalytic characteristics. And small nanocluster catalyst has shown very good catalytic activity in many reaction fields. A cluster of several atoms with a few nanometres in size, not a single metal atom, was expected to be the most mass-efficient catalyst [13]. The size tunning can easily control the corresponding structure and electrical properties, thus achieving excellent reaction activity. Castillo et al. [14] studied the electronic structure of Ag, Au, Pt and Pd clusters adsorption on graphene, finding that the conductivity of the system was modified when metallic clusters were adsorbed on pristine graphene. Niu et al. [15] studied CO_2 dissociation over Pt_xNi_{4-x} bimetallic clusters with and without hydrogen sources, being able to reduce costs through the form of clusters or replacing Pt atom with Ni atom, and obtaining good results. Gao et al. [16,17] optimized Ni_n (n = 1–4) clusters on different graphene substrate and systematically investigated the adsorption characteristics of NO and the activation of O_2, obtaining very reliable results with regularities.

Platinum is one of the most widely used elements in the field of catalyst materials, having the advantage of high catalytic activity and selectivity. However, platinum included in PGM (platinum group metal) is expensive and very rare on earth, thus limiting its large-scale

* Corresponding authors.
E-mail addresses: gaozhyan@163.com (Z. Gao), yangwj@ncepu.edu.cn (W. Yang).

https://doi.org/10.1016/j.apsusc.2020.146200
Received 16 December 2019; Received in revised form 6 March 2020; Accepted 23 March 2020
Available online 27 March 2020

development [18]. One point to fulfill the maximum utilization of platinum is investigating small nanoparticles embedded on the substrate with a high surface-to-volume ratio. Furthermore, the catalytic activity of platinum can be regulated due to a combination of quantum size effect, surface site distribution, and localized coordination effect with the reduced particle sizes [19]. So we can select small platinum clusters to control the CO_2 reduction activity from the perspective of size control. Green et al. [20] studied the feature of CO_2 linking with size-selected Pt cluster anions, stating that CO_2 is highly activated on the Pt_4^- cluster. Chen et al. [21] performed the hydrogen storage on Pt_4-GN through DFT calculation, obtaining reliable results and considering Pt_4 cluster on the B doped graphene as a potential material. As a result, the platinum cluster consists of four Pt atoms has a stable structure, sufficient adsorption sites, and appropriate calculation time [22], so it is feasible enough to be chosen as the catalyst component.

Graphene-based materials are outstanding substrates due to their high electrical conductivity [23], high specific surface area [24], and excellent mechanical properties [25–27]. What needs to be considered is that metal atoms exhibit weak adsorption with the lattice of carbon atoms, leading to the changed electronic structure. Because of the strong sp^2-hybridized binding in the carbonaceous substrate, the interaction between metal atoms and the pristine graphene is weak [28]. Based on this, single vacancy graphene is used to better anchor platinum cluster for the sake of obtaining a catalyst which is stable enough to complete the reaction. Fampiou [29] summarized the structural, electronic and catalytic properties of graphene-supported platinum nanoclusters and part of the article suggests that defect engineering of graphene could be able to enhance the catalytic activity of ultra-small Pt clusters. Tang et al. [30] investigated the catalytic oxidation of CO on Pt/X-graphene(X represents pristine or single vacancy), finding that a vacancy defect in graphene powerfully stabilizes the Pt adatom and makes the Pt atom more positively charged, which helps to weaken the CO adsorption and enhances the O_2 adsorption. Yoo et al. [31] experimentally prepared the Pt clusters supported on graphene from a mixture of [Pt $(NO_2)_2{\cdot}(NH_3)_2$] and GNS powder, finding that GNS indeed gives rise to an extraordinary modification to the properties of Pt clusters and Pt/GNS unfolded unusually high activity as catalyst.

Due to the blank research of the hydrogenation of CO_2 to formic acid over platinum cluster doped defective graphene, the reaction mechanism of CO_2 by H_2 on Pt_4/SV has aroused our interest. In this work, we studied the hydrogenation reduction of CO_2 on the surface of Pt_4/SV by using density functional theory (DFT) calculation. Firstly, an absolutely stable and reliable catalyst model was constructed by structural optimization and the projected density of states (PDOS) analysis. Secondly, the adsorption characteristic of relevant gases was analyzed to lay the foundation for the initial states of the subsequent reaction. Thirdly, the reaction pathways were explored according to the reaction mechanism [32–34] of Langmuir-Hinshelwood (L-H), Eley-Rideal (E-R) and termolecular Eley-Rideal (TER). Then, the kinetic analysis was performed to evaluate the reaction rate of reduction and product desorption under the given temperature range. Finally, the potential effect of the CO molecule was also considered in this study. This work can provide a more deep and systematic understanding on the hydrogenation of CO_2 to formic acid over platinum cluster doped defective graphene, so as to obtain innovative breakthroughs on a new catalyst with efficiency and application value for the reduction of CO_2.

2. Method

Density functional theory (DFT), which is one of the most common and general methods in computational physics and chemistry [35,36], has been adopted to investigate the CO_2 hydrogenation over the platinum cluster deposited on the single vacancy site of the graphene sheet (Pt_4/SV). Vienna ab initio simulation package software (VASP 5.4.4) was used in this work [37,38]. The Projector-Augmented-Wave (PAW) potential described the interaction between nucleus and valence electrons, and the method of Perdew-Burke-Ernzerhof (PBE) was used to describe the related electron exchange energy [39,40]. Based on our previous study [41], a 4 × 4 single-layer graphene was selected as the substrate which was a periodic boundary model. To prevent the effect of mirror images, the vacuum layer was set to 15 Å and the lattice parameter was calculated to 2.48 Å which was consistent with the previous results both in theoretical and experimental aspects [42,43]. The cutoff energy of the plane wave base set used in the relaxation calculation of geometric optimization was set to 500 eV [44]. Comparing static calculation by testing different k-point segmentation from small to large. When the energy change is less than 10 meV per atom, the density of k-point is enough. The Gaussian smearing was set to 0.05 eV [45], and the maximum ionic force was less than 0.02 eV/Å with a 7 × 7 × 1 Γ-centered k-point grid considering the computational time and accuracy [46]. The self-consistent total energy calculation and the density of states calculation adopted denser k-point of 15 × 15 × 1, and the convergence standard of the self-consistent electron iteration was set to 10^{-5} eV. Besides, the ISPIN was set to 2 for spin-polarized calculations [47].

To search for the transition states, the climbing-image nudged elastic band (CI-NEB) for roughly search and the dimer method (IDM) for the accurate search were adopted [48,49]. And the force convergence was 0.1 and 0.05 eV/Å, respectively. The vibration frequency was operated under limited displacements of ± 0.02 Å. Besides, the zero-point energy correction from vibrational frequency was calculated to obtain the accurate system energy. In theory, there was only one imaginary frequency in transition state structures, while there was no imaginary frequency in the most stable structures.

The binding energy (E_{bind}) of Pt_4 cluster on single vacancy graphene was calculated as follows [50]:

$$E_{bind} = E_{sur+Pt_4} - E_{sur} - E_{Pt_4} \quad (1)$$

The cohesive energy (E_{coh}) of Pt_4 cluster, which was used to determine whether atoms are reunited, was calculated as follows:

$$E_{coh} = (E_{Pt_4} - 4{\bullet}E_{Pt})/4 \quad (2)$$

where E_{Pt_4}, E_{Pt} represent the total energies of Pt_4 cluster and the isolated Pt atom respectively.

The adsorption energy (E_{ads}) of gases on Pt_4/SV catalyst, which was used to measure the adsorption strength between the adsorbent and adsorbate, was calculated as follows [11]:

$$E_{ads} = E_{tot} - E_{sur+Pt_4} - E_{gas} \quad (3)$$

where E_{tot}, E_{sur+Pt_4} and E_{gas} represents the total energy of the adsorption system, catalyst, and gases respectively. When the value of E_{ads} is more negative, the adsorption interaction is more stable.

The energy barrier (E_b) and reaction heat (ΔE) for describing the reaction steps were calculated as follows [50,51]:

$$E_b = E_{TS} - E_{IS} \quad (4)$$

$$\Delta E = E_{IM} - E_{IS} \quad (5)$$

where E_{IS}, E_{IM} and E_{TS} represents the energy of the initial state, intermediate state, and transition state respectively in the reaction process.

Kinetic analysis on each reaction pathway was conducted by conventional transition state theory (TST), shown as follows [41]:

$$K^{TST} = \frac{k_B T}{h} \times exp\left(\frac{-\Delta G_b}{k_B T}\right) \quad (6)$$

where K^{TST} is the reaction rate constant; k_B is the Boltzmann constant, 8.62 × 10^{-5} eV•k^{-1}; T is the Kelvin temperature, k; h is the Planck constant, 6.58 × 10^{-16} eV • s; ΔG_b is the energy barrier in Gibbs energy, eV.

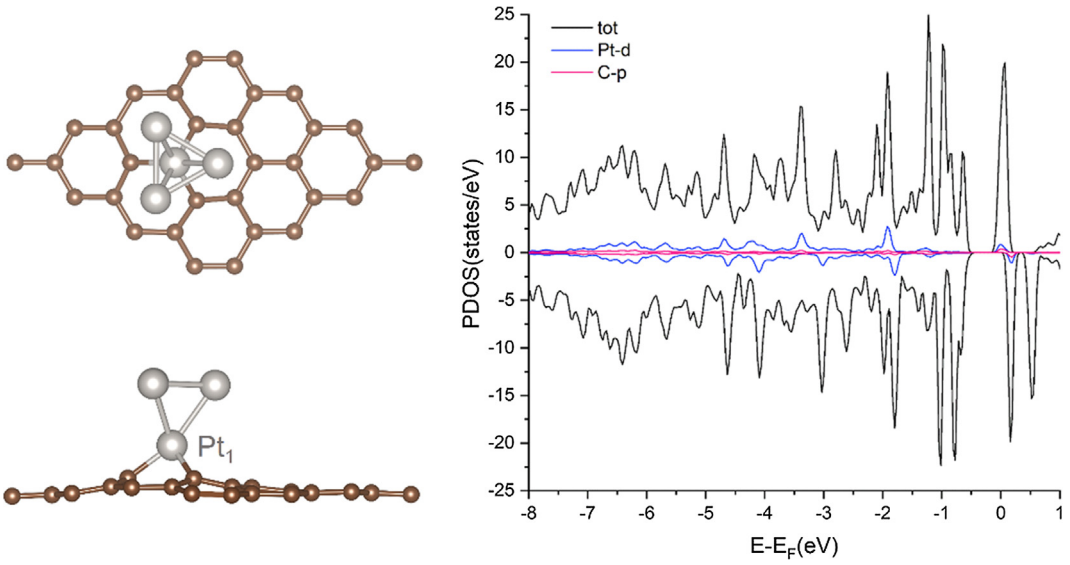

Fig. 1. The geometric structure and PDOS plot of Pt_4/SV.

3. Results and discussion

3.1. Catalyst model

Fig. 1 shows the most stable geometric structure and PDOS plot of Pt_4/SV-GN. Four Pt atoms make up a tetrahedron which locates on the single vacancy site of the graphene, and the bottom Pt atom forms three covalent bonds with neighboring C atoms on the defective graphene. As Table 1 indicates, the average bond length among four Pt atoms is 2.59 Å, and the height between the bottom Pt atoms and the left-most dangling C atoms is 1.97 Å. The average height of the Pt cluster from the graphene surface is 1.82 Å. Electrons of these Pt atoms prefer to transfer to the surface, resulting in a positive charge transfer of 9.54 e in the Pt_4 cluster. According to our calculations, the binding energy of Pt_4 cluster and graphene system is −7.09 eV, consistent with the value of −7.11 eV in the work of Qi et al. [52]. And the cohesive energy of Pt_4 cluster is −2.64 eV, also consistent with −2.68 eV in the work of Munieswaran et al[53]. It is concluded that the binding energy is much larger than the cohesive energy. So the Pt atoms will not reunite which indicates that the Pt_4 cluster can be formed and is stable enough to be anchored. In order to deeply and more qualitatively understand the binding energy, the electronic characteristics of Pt_4/SV are investigated through analyzing the projected density of states (PDOS) of Pt_4 on defective graphene as shown in Fig. 1. DOS performs the states that can be occupied by electrons in the corresponding energy level, while PDOS represents the contribution of each level to some specific atomic orbit. Pt-5d orbit overlaps well with 2p orbit of the C atom around the vacancy according to the peaks below the Fermi level ($E - E_F = 0$), leading to the strong interaction of Pt_4 cluster anchored on the single vacancy graphene. In conclusion, Pt_4/SV-GN selected in this work is stable enough to catalyze the hydrogenation of carbon dioxide.

3.2. Gas adsorption

The most stable adsorption structures of H_2, CO_2, H_2 + CO_2, and $2CO_2$ are shown in Fig. 2. And the key parameters in the process of gas adsorption are concluded in Table 2. From Table 2, Δh represents the height from bottom Pt atom to the leftmost C atom, using the same criteria as described above. The bottom Pt atom does not have an obvious uplift in the process of gas adsorption. Besides, the bond length of H_2 has an obvious elongation compared with that in individual H_2 molecule (0.75 Å), declaring a strong activation of H_2 after adsorption. Activated H_2 as a reductant is very helpful in the subsequent reduction of CO_2. The average bond length of CO_2 elongates just a little compared with that in individual CO_2 molecule (1.25 Å), maybe owing to it that CO_2 molecule is too stable to activate. In the work of Xu et al [54], the adsorption energy of CO_2 on Ni_4/SV has a large value of −2.72 eV, which may result in the situation that CO_2 is adsorbed on catalyst surface too strongly to partake in reaction. The charges transfer of Pt_4 cluster, single vacancy graphene, and adsorbed gas are summarized, respectively. After adsorption, Pt_4 cluster and defective graphene substrate always gain electrons, while the gases always lose electrons.

From the analysis of gas adsorption, the reaction mechanism of CO_2 reduction can be guided. The adsorption energy of H_2 on Pt_4/SV is relatively greater than CO_2 on Pt_4/SV, so we consider the CO_2 gas molecule reacts with the adsorbed H_2 on Pt_4/SV in the E-R mechanism. The coadsorption energy of H_2 and CO_2 is much higher than the individual H_2 or CO_2, so the L-H mechanism should not be ignored. The adsorption of double CO_2 is also relatively strong, so the reaction between double CO_2 gas molecules and the adsorbed H_2 is also considered on the basis of TER mechanism.

Table 1
The bond length of Pt−Pt and Pt−C, the height, the charge, the cohesive energy and binding energy of Pt_4/SV.

Catalyst	d_{Pt-Pt} (Å)	d_{Pt-C}(Å)	h(Å)	q(e)	E_{coh}(eV)	E_{bind}(eV)
Pt_4/SV	2.59	1.97	1.82	9.54	−2.64	−7.09

3.3. Reaction path analysis for the CO_2 hydrogenation

3.3.1. E-R reaction mechanism

E-R reaction is the reaction mechanism between gaseous molecules and the adsorbed particles. Two different pathways performed in this work classified according to the different atom in CO_2 conquered by H_2. Path 1 follows the pathway that CO_2 conquers the bond of two hydrogen atoms as shown in Fig. 3. The carbon atom of CO_2 first combines with H_2 and intermediate COOH forms on the Pt_4/SV. This step is exothermic and releases the energy of 0.15 eV. In this process, the bond length of H_2 elongates from 1.98 Å (IS1) to 2.11 Å (TS1), and the CO_2 molecule is also elongating to some extent. The energy barrier is 1.01 eV being overcome in the first step. Then, one oxygen atom of adsorbed COOH combines with the residual hydrogen atom in order to form HCOOH at last. This second step is endothermic with the adsorbed energy of 0.69 eV, and the energy barrier is 1.28 eV across from the

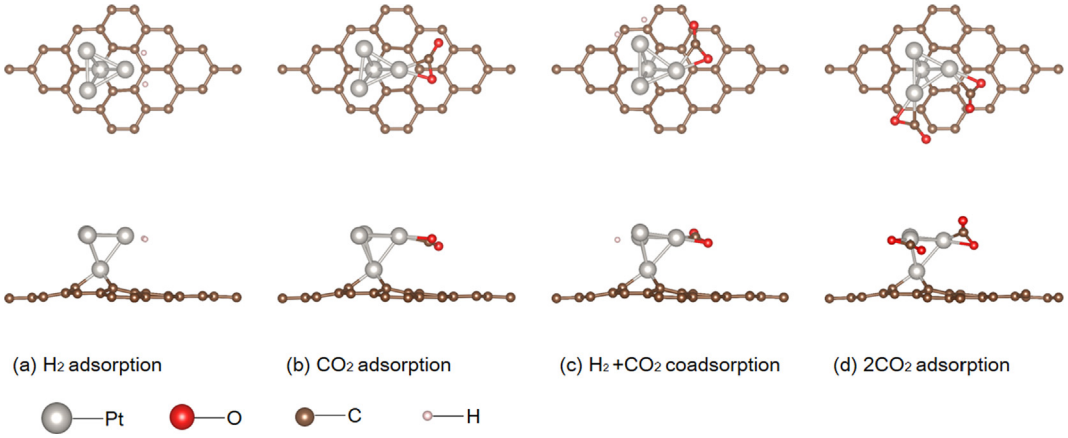

Fig. 2. The adsorption configurations of different gases on Pt_4/SV (top and side views).

Table 2
The height of Pt_4 cluster (Δh, Å), the relevant bond length(Å), charge transfer (Δq, e), and adsorption energy (E_{ads}, eV) in the gas adsorption.

Adsorbate	Δh(Å)	d(Å)		Δq_{Pt4}(e)	Δq_{sub}(e)	Δq_{gas}(e)	E_{ads}(eV)
H_2	1.79	h-h	1.96	0.12	−0.17	0.08	−1.79
CO_2	1.80	C−O	1.25	−0.21	−0.25	0.51	−1.07
H_2 + CO_2	1.79	h-h/C−O	1.91/1.24	−0.06	−0.26	0.37	−2.58
$2CO_2$	1.79	C−O	1.24	−0.38	−0.31	0.76	−1.64

COOH to the formic acid, thus being a rate-determining step. Compared with the energy barrier of 1.38 eV through the same reaction pathway on Cu/SV [55] (Cu atom embedded on the single vacancy graphene), some improvement happens here.

Path 2 also follows the pathway that CO_2 conquers the bond of two hydrogen atoms as shown in Fig. 4. But different from path 1, the oxygen atom of CO_2 first combines with hydrogen and intermediate HCOO forms on the Pt_4/SV. There are three steps and three transition states in this pathway. The first step is endothermic with the adsorbed energy of 0.48 eV, and the energy barrier is 1.64 eV. Compared with the value of 1.73 eV through the same pathway on Cu/SV, HCOO is relatively easy to form on Pt_4/SV. Sirijaraensre [55] used another H_2 molecule to achieve the next step with the energy barrier of 0.46 eV. In this work, only one H_2 molecule used in the whole reaction process, thus saving input materials. HCOO switches from vertical structure to parallel structure to be more convenient to combine with the residual hydrogen atom with the released energy of 0.26 eV and energy barrier of 0.23 eV (IM2 → IM3). Parallel HCOO links with the oxygen atom through crossing the energy barrier of 0.66 eV, being endothermic by 0.31 eV (IM3 → FS1)

3.3.2. L-H reaction mechanism

An alternative pathway for CO_2 reduction was investigated in the L-H mechanism through path 3 as shown in Fig. 5. L-H is the catalytic mechanism of surface reaction with two adsorbed molecules. IS represents the initial state that H_2 and CO_2 are both adsorbed on Pt_4/SV, and these two adsorbed molecules react to form COOH (IM4). The reaction heat is 0.54 eV and the energy barrier is 0.72 eV. COOH subsequently combines with the residual hydrogen atom, thus obtaining HCOOH (IM4 → FS1). This second step is also endothermic by 0.76 eV and needs to cross the energy barrier of 3.11 eV. It is a relatively large energy barrier, thus making the reaction hard to happen through the L-H mechanism. It may be the reason that there is very rare literature investigating CO_2 reduction using L-H mechanism.

3.3.3. TER reaction mechanism

TER reaction is the termolecular reaction mechanism between two gaseous molecules and the adsorbed particles. In this work, the activated H_2 molecule is first adsorbed on Pt_4/SV with the Pt-H of 1.57 Å, and the two CO_2 gases intend to react with H_2 leaving the Pt-C of 3.65/3.60 Å. The two CO_2 conquered one hydrogen atom respectively, thus forming two COOH with the Pt-C of 2.00/1.97 Å as shown in FS2 from Fig. 6. FS2 adsorbs another new H_2 molecule to form IS4, and the bond

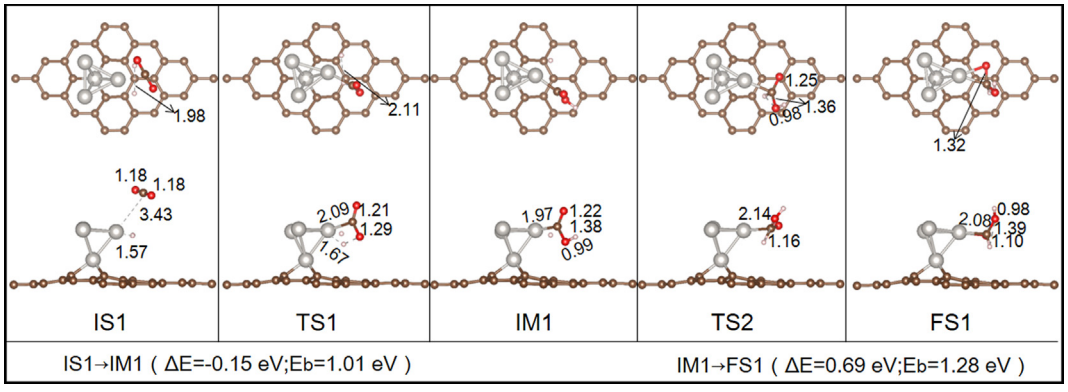

Fig. 3. CO_2 reduction reaction configurations in E-R mechanism through path 1 (top and side views).

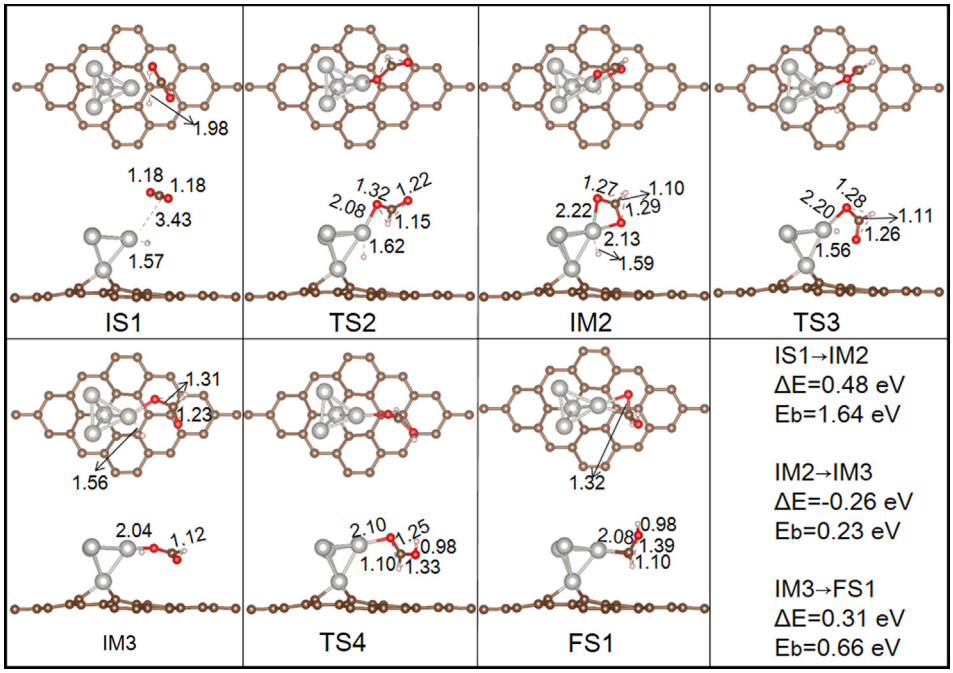

Fig. 4. CO_2 reduction reaction configurations in E-R mechanism through path 2 (top and side views).

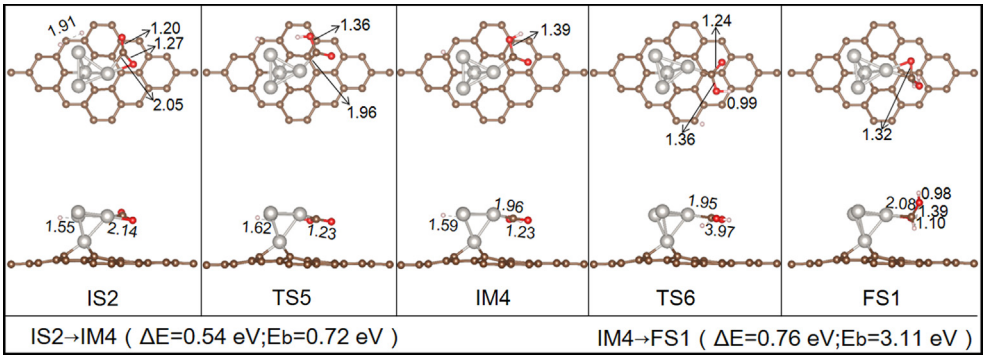

Fig. 5. CO_2 reduction reaction configurations in the L-H mechanism through path 3 (top and side views).

length between the Pt atom and the bottom hydrogen atom is 2.80 Å. Similar as the first step, two COOH conquered one hydrogen atom respectively, thus forming two HCOOH with the Pt-O of 2.09/2.11 Å. These two steps are both exothermic with the released energy of 0.25 eV and 0.02 eV respectively. The energy barrier is relatively small with a value of 0.16 eV and 0.53 eV, making the second step become the rate-determining step. Esrafili et al. [56] investigated the termolecular mechanism of CO_2 reduction by H_2 molecule over Pt-G (single Pt atom embedded on single vacancy graphene), and the first step is the rate-determining step with the energy barrier of 1.15 eV. In conclusion, TER mechanism of CO_2 reduction by H_2 has a great advantage in terms of Pt_4/SV catalysts.

3.3.4. Energy profiles analysis

The energy profiles through different pathways were plotted in Fig. 7, and the total energy of substances was performed as zero-point energy. The CO_2 hydrogenation through distinct pathways can be envisioned as the following sequence steps:

$$CO_2 + H_2^* \rightarrow COOH^*/OCOH^* + H^* \rightarrow HCOOH \quad (7)$$

$$CO2^* + H_2^* \rightarrow COOH^* + H^* \rightarrow HCOOH \quad (8)$$

$$2CO_2 + H_2^* \rightarrow 2COOH^*, H_2 + 2COOH^* \rightarrow 2HCOOH \quad (9)$$

Path 1 and path 2 in the E-R mechanism were described by formula (6), plotted in Fig. 7(a). Along the same starting and ending points (IS1 → FS1), the two pathways absorb the same heat of 0.53 eV. But during the first step of adding one H atom, path 1 crosses the energy barrier of 1.01 eV, lower than path 2 with the value of 1.64 eV. In the second step of adding another H atom, path 2 experiences two transition states with the energy barrier of 0.23 eV and 0.66 eV, much lower than path 1 with 1.28 eV which has one transition state. Path 3 in the L-H mechanism was described by formula (7), plotted in Fig. 7(a). The whole heat absorbed is 1.4 eV (IS2 → FS1). Adding the first H atom needs overcoming the energy barrier of 0.72 eV, lower than adding the second H atom with the value of 3.11 eV. In view of these analyses, in the CO_2 reduction reaction through the bimolecular mechanism, the E-R mechanism reaction is more likely to happen than the L-H mechanism reaction.

Path 4 in TER mechanism was described by formula (8), plotted in Fig. 7(b). The whole journey released the heat of 0.27 eV (IS3 → FS3). Adding one H atom on each CO_2 molecule is very easy to happen with the energy barrier of 0.16 eV, and adding residual H atoms conquers the similarly small value of 0.53 eV. From this point of view, CO_2 reduction reaction through TER mechanism is more likely to happen than other mechanisms.

From Fig. 7, we can clearly find that the desorption energy barrier of HCOOH through path 1/ 2/ 3 is 1.12 eV, lower than the energy barrier

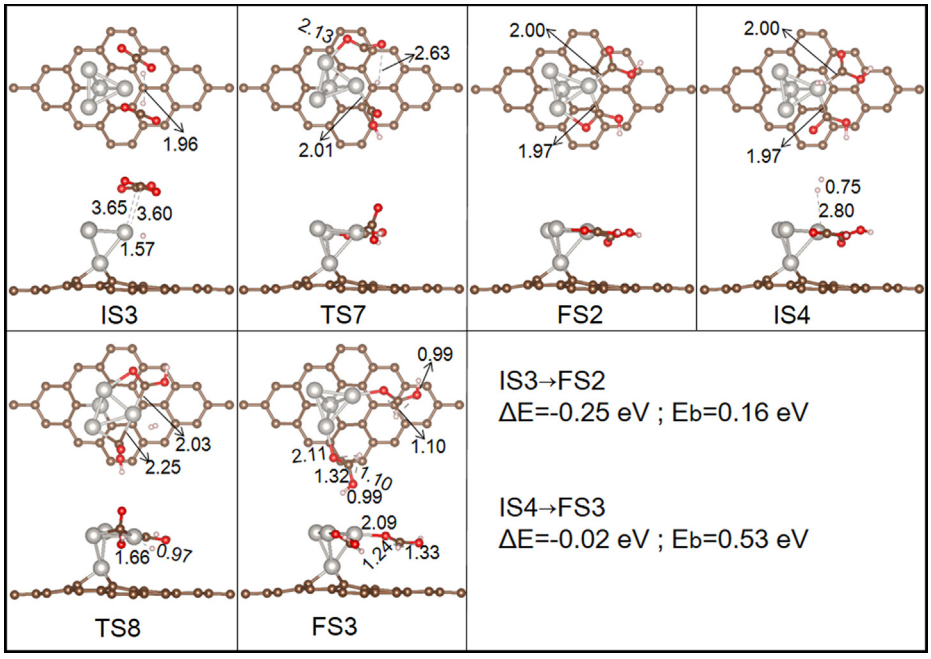

Fig. 6. CO_2 reduction reaction configurations in TER mechanism through path 4 (top and side views).

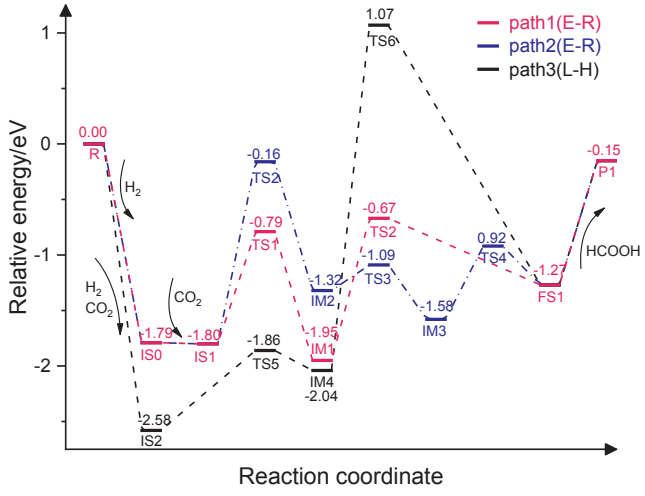

(a) Energy profile of CO_2 hydrogenation in E-R and L-H mechanism

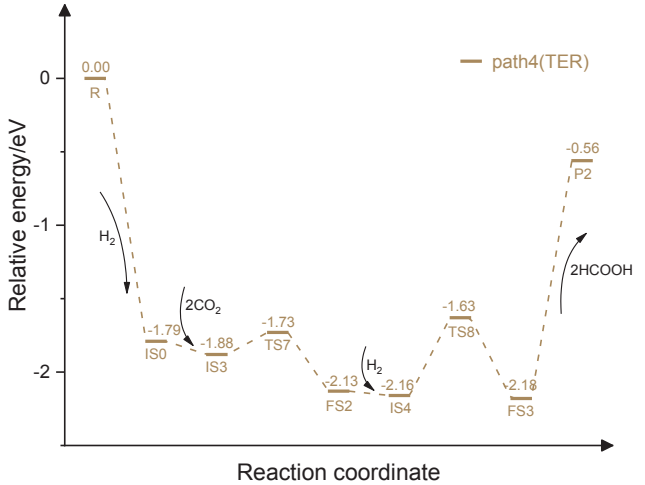

(b) Energy profile of CO_2 hydrogenation in TER mechanism

Fig. 7. Energy profiles of CO_2 hydrogenation.

of rate-determining step in CO_2 hydrogenation, especially through path 3. However, the desorption energy barrier through path 4 is 1.62 eV, higher than that in CO_2 hydrogenation. After the release of HCOOH from the catalyst, the Pt_4 cluster deposited on the single vacancy graphene (R) is also used as the catalyst for the next cycle of CO_2 hydrogenation.

3.4. Kinetic analysis

In order to evaluate the Pt_4/SV catalyst according to the speed of catalytic reduction, the kinetic analysis was considered in this work to study the kinetic characteristics of different reaction pathways. Rate-determining steps of these four pathways should be selected to representatively perform kinetic analysis. Specifically, choices can be made as follows: IM1 → FS1 (path 1), IS1 → IM2 (path 2), IM4 → FS1 (path 3), IS4 → FS3 (path 4). Because the energy barriers of desorption process were relatively large, two kinds of desorption steps (FS1 → P1, FS2 → P2) were also selected in this work. According to the conventional transition state theory, the reaction rate constant can be acquired, as shown in Fig. 8. According to the linear fitting of the reaction rate constants, the corresponding activation energy (E_a) and pre-exponential factor (A) of rate-determining steps from different reduction pathways concluded in Table 3.

From Fig. 8, the reaction rate constants increase with the temperature rise, indicating that higher temperature accelerates the reaction rate of reduction and desorption processes. Among them, path 4 has a very high reaction rate constants compared with other processes. Path 3 has a relatively low reaction rate constants. However, the change is still quick, meaning that a small temperature rise can achieve a large reaction rate increase. Furthermore, the activation energy ranges from 0.56 eV to 2.81 eV, confirming that these four reduction pathways and the desorption process can be relatively easy to happen. Among them, the activation energy of CO_2 hydrogenation in path 4 is only 0.56 eV, indicating that the hydrogenation of CO_2 is very easy to happen, thereby achieving a better reduction result. And the CO_2 reduction reaction through path 4 can take place spontaneously at the given temperature range. In contrast, the activation energy in path 3 is 2.81 eV and the corresponding reaction rate is slowest which means that CO_2 reduction through this pathway is relatively hard to occur.

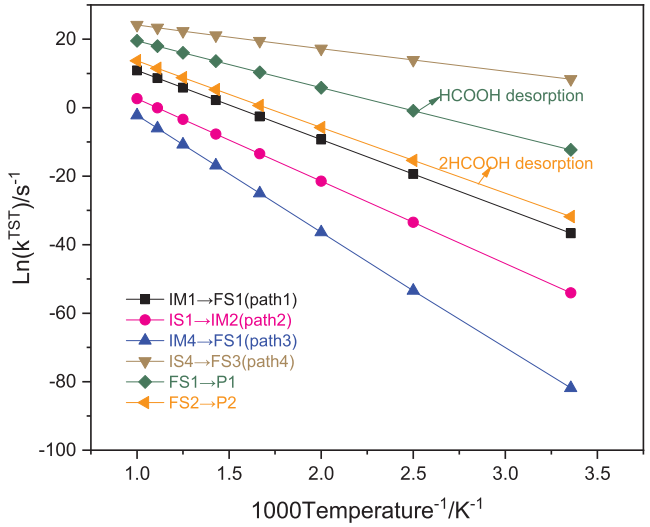

Fig. 8. The logarithm of reaction rate constants of reduction and desorption processes.

Table 3
The kinetic parameters of different processes.

Processes	E_a (eV)	A (s^{-1})
IM1 → FS1(path1)	1.68	3.04×10^{13}
IS1 → IM2(path2)	2.00	3.84×10^{11}
IM4 → FS1(path3)	2.81	4.77×10^{13}
IS4 → FS3(path4)	0.56	2.01×10^{13}
FS1 → P1	1.12	1.98×10^{14}
FS2 → P2	1.61	1.98×10^{14}

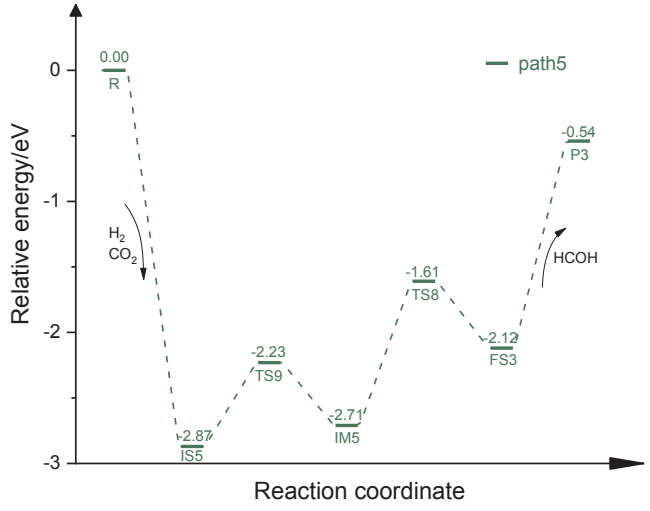

Fig. 9. Energy profile of CO hydrogenation.

Combined with the above analysis, the hydrogenation of CO_2 follows TER as the main reaction mechanism, partially following the E-R mechanism, and the reaction follows the L-H mechanism with difficulties.

3.5. The effect of CO molecule

Considering that CO molecule may be the most significant impact on the reduction of CO_2, CO reduced by H_2 should be investigated in this work. Formula (9) reveals the reaction steps gradually. Fig. 9 shows the specific reaction processes including the corresponding energies.

$$CO^* + H_2^* \rightarrow HCO^* + H^* \rightarrow HCOH \quad (10)$$

We optimized the stable configuration of CO adsorbed on Pt_4/SV, demonstrating a kind of strong chemisorption with the adsorption energy of −2.87 eV (Fig. S1). Taking into account this competitive adsorption, the reaction pathway of CO hydrogenation was calculated, as shown in Fig. 9. Besides, the specific configurations, corresponding bond length, reaction heat, and energy barrier were shown in Fig. S2. H_2 and CO coadsorb strongly (-2.87 eV) and carry out the first reaction step with the heat absorption of 0.16 eV, and the energy barrier is 0.64 eV. HCO combines with the residual H atom to form the final state (HCOH), being endothermic by 0.59 eV and crossing the energy barrier of 1.11 eV. For the relatively large desorption energy of 1.58 eV, the HCOH molecule cannot release from the surface easily at the ambient situation.

4. Conclusions

In this work, adsorption characteristics and reaction processes of CO_2 and H_2 were investigated systematically adopting Pt_4/SV-GN catalyst with the computing way of density functional theory which may help to open up another dimension for the rational design of CO_2 hydrogenation catalyst. After performing gas adsorption, reaction path analysis, kinetic analysis, and CO effect analysis, we gain the following results:

(1) Pt_4/SV-GN is a feasible catalyst which can be firmly formed and has a moderate adsorption effect on gases, especially on a single gas molecule.
(2) The hydrogenation of CO_2 on the catalyst can occur easily through path 1/ 2/ 4 following E-R and TER mechanism with the rate-determining step energy barriers of 1.28 eV, 1.64 eV, and 0.53 eV. Contrarily, reaction occurs hard through path 3 following L-H mechanism with the value of 3.11 eV.
(3) Release of one HCOOH molecule and two HCOOH molecules can achieve with the desorption energy of 1.12 eV through path 1/ 2/ 3 and 1.62 eV through path 4.
(4) Kinetic analysis calculated the reaction rates of considered processes, confirming that the steps especially IS4 → FS3, are fast enough to ensure normal processes under different temperatures.
(5) H_2 and CO coadsorb too strongly on Pt_4/SV-GN (−2.87 eV) and the energy barrier of the rate-determining step is 1.11 eV. And HCOH molecule releases from the surface with the desorption energy of 1.58 eV.

CRediT authorship contribution statement

Ge Yan: Investigation. **Zhengyang Gao:** Resources, Supervision. **Mingliang Zhao:** Visualization. **Weijie Yang:** Validation. **Xunlei Ding:** Methodology.

Acknowledgments

This work was supported by the Beijing Municipal Natural Science Foundation (2182066), Natural Science Foundation of Hebei Province of China (B2018502067) and the Fundamental Research Funds for the Central Universities (JB2015RCY03 and 2017XS121).

Appendix A. Supplementary material

Supplementary data to this article can be found online at https://doi.org/10.1016/j.apsusc.2020.146200.

References

[1] D. Cheng, F.R. Negreiros, E. Apra, A.J.C. Fortunelli, Computational approaches to the chemical conversion of carbon dioxide, ChemSusChem 6 (2013) 944–965.
[2] M.A.A. Sheha, C.P.J.A. Tsokos, C. Sciences, Statistical modeling of emission factors

of fossil fuels contributing to atmospheric carbon dioxide in Africa, Atmos. Climate Sci. 9 (2019) 438–455.
[3] P.G. Jessop, Greenhouse gas carbon dioxide mitigation: science and technology by Martin M. Halmann (Weizmann Institute of Science, Israel) and Meyer Steinberg (Brookhaven National Laboratory). Lewis Publishers: Boca Raton, FL. 1999. xix + 568 pp. 9.95. ISBN 1-56670-284-4, J. Am. Chem. Soc. 123 (2001) 7197-7197.
[4] Y. Li, S.H. Chan, Q.S.J. Nanoscale, ChemInform abstract: heterogeneous catalytic conversion of CO_2: a comprehensive theoretical review, Nanoscale 7 (2015) 8663–8683.
[5] P.G. Jessop, T. Ikariya, R. Noyori, Homogeneous hydrogenation of carbon dioxide, Chem. Rev. 26 (2010) no-no.
[6] C. Liu, T.R. Cundari, N.J. De Yonker, M.L. Drummond, J.J. Determan, CO2 reduction on transition metal (Fe Co, Ni, and Cu) surfaces. in comparison with homogeneous catalysis, J. Phys. Chem. C 116 (2012) 5681–5688.
[7] Y. Yuan, H. You, L. Ricardez-Sandoval, Recent advances on first-principles modeling for the design of materials in CO2 capture technologies, Chin. J. Chem. Eng. 27 (2018) 1554–1565.
[8] G. Peng, S. Sibener, G.C. Schatz, S.T. Ceyer, M. Mavrikakis, CO_2 hydrogenation to formic acid on Ni (111), (2012) 1163001–1163006.
[9] W. Xu, L. Ma, B. Huang, X. Cui, X. Niu, H. Zhang, Thermodynamic analysis of formic acid synthesis from CO_2 hydrogenation, in: 2011 International Conference on , Materials for Renewable Energy & Environment, 2011, pp. 1473–1477.
[10] Yan Jiao, Aijun Du, Zhonghua Zhu, Victor Rudolph, Gao Qing (Max) Lu, Sean C. Smith, A density functional theory study on CO_2 capture and activation by graphene-like boron nitride with boron vacancy, Catalysis Today 175 (1) (2011) 271–275, https://doi.org/10.1016/j.cattod.2011.02.043.
[11] P. Cabrera-Sanfelix, Adsorption and reactivity of CO_2 on defective graphene sheets 113 (2009) 493–498.
[12] He Xu, Wei Chu, Wenjing Sun, Chengfa Jiang, Zhongqing Liu, DFT studies of Ni cluster on graphene surface: effect of CO2 activation, RSC Adv. 6 (99) (2016) 96545–96553, https://doi.org/10.1039/C6RA14009B.
[13] A. Beniya, S. Higashi, Towards dense single-atom catalysts for future automotive applications, Nature Catal. 2 (2019) 590–602.
[14] R.M. Del Castillo, L.E. Sansores, Study of the Electronic Structure of Ag, Au, Pt and Pd clusters adsorption on graphene and their effect on conductivity 88 (2015) 248.
[15] Juntian Niu, Jingyu Ran, Zhiliang Ou, Xuesen Du, Ruirui Wang, Wenjie Qi, Peng Zhang, CO_2 dissociation over Pt_xNi_{4-x} bimetallic clusters with and without hydrogen sources: A density functional theory study, J. CO2 Utilizat. 16 (2016) 431–441, https://doi.org/10.1016/j.jcou.2016.10.008.
[16] Z. Gao, A. Li, X. Liu, C. Ma, X. Li, W. Yang, X. Ding, Density functional study of the adsorption of NO on Ni_n (n = 1, 2, 3 and 4)clusters doped functionalized graphene support, Appl. Surf. Sci. 481 (2019) 940–950.
[17] Z. Gao, A. Li, X. Li, X. Liu, C. Ma, J. Yang, W.H.Li Yang, The adsorption and activation of oxygen molecule on nickel clusters doped graphene-based support by DFT, Mol. Catal. 477 (2019) 110547.
[18] A. Bruix, Y. Lykhach, I. Matolínová, A. Neitzel, T. Skála, N. Tsud, M. Vorokhta, V. Stetsovych, K. Ševčíková, J. Mysliveček, Maximum noble-metal efficiency in catalytic materials: atomically dispersed surface, Platinum 53 (2014) 10525–10530.
[19] Lin Li, Ask H. Larsen, Nichols A. Romero, Vitali A. Morozov, Christian Glinsvad, Frank Abild-Pedersen, Jeff Greeley, Karsten W. Jacobsen, Jens K. Nørskov, Investigation of catalytic finite-size-effects of platinum metal clusters, J. Phys. Chem. Lett. 4 (1) (2013) 222–226, https://doi.org/10.1021/jz3018286.
[20] Alice E. Green, Jasmin Justen, Wieland Schöllkopf, Alexander S. Gentleman, André Fielicke, Stuart R. Mackenzie, IR signature of size-selective CO2 activation on small platinum cluster anions, Angew. Chem. Int. Ed. 57 (45) (2018) 14822–14826, https://doi.org/10.1002/anie.201809099.
[21] I.-N. Chen, S.-Y. Wu, H.-T. Chen, Hydrogen storage in N-and B-doped graphene decorated by small platinum clusters: a computational study, Appl. Surf. Sci. 441 (2018) 607–612.
[22] Y. Tang, Z. Yang, Nanoscience, nanotechnology, the formation and properties of Pt-4 clusters on the defective graphene, support 13 (2013) 1612–1615.
[23] X. Liu, T. Xu, Y. Li, Z. Zang, X. Peng, H. Wei, W. Zha, F. Wang, Enhanced X-ray photon response in solution-synthesized CsPbBr 3 nanoparticles wrapped by reduced graphene oxide, Sol. Energy Mater. Sol. Cells 187 (2018) 249–254.
[24] W. Wu, Q. Yu, P. Peng, Z. Liu, J. Bao, S.S. Pei, Control of thickness uniformity and grain size in graphene films for transparent conductive electrodes, Nanotechnology 23 (2012) 035603.
[25] D. Deng, K.S. Novoselov, Q. Fu, N. Zheng, Z. Tian, X. Bao, Catalysis with two-dimensional materials and their heterostructures 11 (2016) 218.
[26] V. Georgakilas, J.N. Tiwari, K.C. Kemp, J.A. Perman, A.B. Bourlinos, K.S. Kim, R. Zboril, Noncovalent functionalization of graphene and graphene oxide for energy materials, biosensing, catalytic, and biomedical applications 116 (2016) 5464–5519.
[27] K.S. Novoselov, Graphene: Materials in the Flatland 25 (2011) 4081–4106.
[28] Y.N. Tang, C.G. Li, W.G. Chen, X.Q. Dai, Geometric stability, electronic structure and reactivity of Pt4 cluster supported on defective graphene 159 (2015) 57–65.
[29] I. Fampiou, Structural, Electronic and Catalytic Properties of Graphene-supported Platinum Nanoclusters, Doctoral Dissertations 185 (2014).
[30] Y. Tang, Z. Yang, X. Dai, A theoretical simulation on the catalytic oxidation of CO on Pt/graphene 14 (2012) 16566–16572.
[31] E. Yoo, T. Okata, T. Akita, M. Kohyama, J. Nakamura, I. Honma, Enhanced electrocatalytic activity of Pt subnanoclusters on graphene nanosheet, Surface 9 (2009) 2255–2259.
[32] K.V. Kumar, K. Porkodi, F. Rocha, Langmuir–Hinshelwood kinetics – a theoretical study 9 (2008) 82–84.
[33] A.J. Farebrother, A.J.H.M. Meijer, D.C. Clary, A.J. Fisher, Formation of molecular hydrogen on a graphite surface via an, Eley-Rideal mechanism 319 (2000) 303–308.
[34] G. Xu, R. Wang, F. Yang, D. Ma, Z. Yang, Z. Lu, CO oxidation on single Pd atom embedded defect-graphene via a new termolecular Eley-Rideal mechanism, Carbon 118 (2017) 35–42.
[35] Zhengyang Gao, Xiaoshuo Liu, Ang Li, Chuanzhi Ma, Xiang Li, Xunlei Ding, Weijie Yang, Adsorption behavior of mercuric oxide clusters on activated carbon and the effect of SO2 on this adsorption: a theoretical investigation, J Mol Model 25 (5) (2019), https://doi.org/10.1007/s00894-019-4026-3.
[36] R.G. Parr, S.R. Gadre, L.J. Bartolotti, Local density functional theory of atoms and molecules 76 (1979) 2522–2526.
[37] G. Kresse, J. Furthmuller, Efficiency of ab-initio total energy calculations for metals and semiconductors using a plane-wave basis, Set 6 (1996) 15–50.
[38] G. Kresse, D. Joubert, From ultrasoft pseudopotentials to the projector augmented-wave method, Physi Rev. B 59 (1999) 1758–1775.
[39] X. Liu, Z. Gao, C. Wang, M. Zhao, X. Ding, W. Yang, Z. Ding, Hg0 oxidation and SO_3, Pb0, PbO, $PbCl_2$ and As_2O_3 adsorption by graphene-based bimetallic catalyst ((Fe, Co)@N-GN): A DFT study, Appl. Surf. Sci. 496 (2019).
[40] G. Kresse, J. Furthmuller, Efficient iterative schemes for ab initio total-energy calculations using a plane-wave basis set, Phys. Rev. B 54 (1996) 11169–11186.
[41] W. Yang, Z. Gao, X. Liu, X. Li, X. Ding, W. Yan, Single-atom iron catalyst with single-vacancy graphene-based substrate as a novel catalyst for NO oxidation: a theoretical study, Catal. Sci. Technol. 8 (2018) 4159–4168.
[42] J.M. Carlsson, M. Scheffler, Structural, electronic, and chemical properties of nanoporous carbon, Phys. Rev. Lett 96 (2006) 046806.
[43] W. Yang, Z. Gao, X. Ding, G. Lv, W. Yan, The adsorption characteristics of mercury species on single atom iron catalysts with different graphene-based substrates, Appl. Surf. Sci. 455 (2018) 940–951.
[44] L. Gong, J.J. Chen, Y. Mu, Catalytic CO_2 reduction to valuable chemicals using NiFe-based nanoclusters: a first-principle theoretical, evaluation 19 (2017) 28344.
[45] K.T. Chan, J.B. Neaton, M.L. Cohen, First-principles study of metal adatom adsorption on graphene 77 (2008) 235430.
[46] H.J. Monkhorst, J.D. Pack, Special points for Brillouin-zone integrations 13 (1976) 5188–5192.
[47] A. Vojvodic, J.K. Norskov, Abild-F. Pedersen, Electronic structure effects in transition metal surface, chemistry 57 (2014) 25–32.
[48] G. Henkelman, B.P. Uberuaga, H. Jonsson, A climbing image nudged elastic band method for finding saddle points and minimum energy paths, J. Chem. Phys 113 (2000) 9901–9904.
[49] A. Heyden, A.T. Bell, F.J. Keil, Efficient methods for finding transition states in chemical reactions: comparison of improved dimer method and partitioned rational function optimization method 123 (2005) 224101.
[50] P. Janthon, S.M. Kozlov, F. Vines, J. Limtrakul, F. Illas, Establishing the accuracy of broadly used density functionals in describing bulk properties of transition metals, Chem. Theory Comput. 9 (2013) 1631–1640.
[51] Z. Gao, X. Liu, A. Li, X. Li, X. Ding, W. Yang, Bimetallic sites supported on N-doped graphene ((Fe,Co)/N-GN) as a new catalyst for NO oxidation: A theoretical investigation, Mol. Catal. 470 (2019) 56–66.
[52] Q. Qi, H. Liu, W. Feng, H. Tian, H. Xu, X. Huang, Theoretical investigation on the interaction of subnano platinum clusters with graphene using DFT, Methods 96 (2015) 268–276.
[53] P. Munieswaran, S. Seenithurai, R.K. Pandyan, S.V. Kumar, C. Saranya, M. Mahendran, A DFT study on the adsorption of CO and CO_2 molecules on Pt4 and Ir4 clusters, in: AIP Conference Proceedings, AIP Conference Proceedings 1665 (2015) 050134.
[54] H. Xu, W. Chu, W. Sun, C. Jiang, Z. Liu, DFT studies of Ni cluster on graphene surface: effect of CO_2 activation, RSC Adv. 6 (2016) 96545–96553.
[55] J. Sirijaraensre, J. Limtrakul, Hydrogenation of CO_2 to formic acid over a Cu-embedded graphene: A DFT, Study 364 (2016) 241–248.
[56] Mehdi D. Esrafili, Fahimeh Sharifi, Leila Dinparast, Catalytic hydrogenation of CO 2 over Pt- and Ni-doped graphene: A comparative DFT study, J. Mol. Graphics Model. 77 (2017) 143–152, https://doi.org/10.1016/j.jmgm.2017.08.016.